Transl Clin Pharmacol. 2022 Mar;30(1):24-36
https://doi.org/10.12793/tcp.2022.30.e4
pISSN 2289-0882·eISSN 2383-5427

Translational and Clinical Pharmacology TCP

Original Article

Check for updates

Physiologically-based pharmacokinetic modeling of nafamostat to support dose selection for treatment of pediatric patients with COVID-19

Yong-Soon Cho [1,2,*] **and Jae-Gook Shin** [1,2]

[1]Center for Personalized Precision Medicine of Tuberculosis (cPMTb), Inje University College of Medicine, Busan 47392, Korea
[2]Department of Pharmacology and Clinical Pharmacology, PharmacoGenomics Research Center, Inje University College of Medicine, Busan 47392, Korea

OPEN ACCESS

Received: Dec 19, 2021
Revised: Feb 14, 2022
Accepted: Feb 25, 2022
Published online: Mar 9, 2022

***Correspondence to**
Yong-Soon Cho
Department of Pharmacology and Clinical Pharmacology, PharmacoGenomics Research Center, Inje University College of Medicine, 75 Bokji-ro, Busanjin-gu, Busan 47392, Korea.
Email: ysncho@gmail.com

ORCID iDs
Yong-Soon Cho
https://orcid.org/0000-0003-1424-1123
Jae-Gook Shin
https://orcid.org/0000-0002-5821-850X

Funding
This work was supported by the National Research Foundation of Korea (NRF) grant funded by the Korean government (MSIT) (No.2018R1A5A2021242) and also supported by the National Research Foundation of Korea (NRF) grant funded by the Korea government (MSIT) (No. 2021R1F1A1056393).

Conflict of Interest
- Authors: Nothing to declare
- Reviewers: Nothing to declare
- Editors: Nothing to declare

ABSTRACT

Pediatric patients with coronavirus disease 2019 (COVID-19) are increasing, and severe cases such as multisystem inflammatory syndrome are being reported. Nafamostat, a repurposing drug, is currently being explored for the treatment of COVID-19 in adults. However, the data supporting its exposure in pediatrics remains scarce. Physiologically-based pharmacokinetic (PBPK) modeling enables the prediction of drug exposure in pediatrics based on ontogeny of metabolic enzymes and age dependent anatomical and physiological changes. The study aimed to establish a PBPK model of nafamostat in adults, then scale the adult PBPK model to children for predicting pediatric exposures of nafamostat and an optimal weight-based nafamostat dose in pediatric population. The developed model adequately described adult exposure data in healthy volunteers following i.v. administration with three doses (10, 20, and 40 mg). Scaling adult PBPK models to five pediatric groups predicted that as age advances from neonate to adult, the exposure of nafamostat slightly increased from neonate to infant, steadily decreased from infant to child, and then increased from child to adult after the administration of 0.2 mg/kg/h for 14 days, a dosing regimen being conducted in a clinical trial for COVID-19. Based on the fold change of predicted area under the curve for the respective pediatric group over those of adults, weight-based dosages for each pediatric group may be suggested. The novel PBPK model described in this study may be useful to investigate nafamostat pharmacokinetics in a pediatric subgroup further.

Keywords: Pharmacokinetics; Nafamostat; Child; COVID-19

INTRODUCTION

The current coronavirus disease 2019 (COVID-19) pandemic has emerged as a critical global health crisis. This disease is caused by severe acute respiratory syndrome coronavirus 2 (SARS-CoV-2). As of November 2021, there have been over 250 million cases and greater than 5 million deaths worldwide (https://coronavirus.jhu.edu/map.html). Although the percentage of COVID-19 diagnosis in children is likely to be lower than that of adults, the incidence of COVID-19 in a pediatric population is not well-known. In South Korea, around 15% of the reported COVID-19 cases occurs in individuals less than 19 years of age (http://ncov.mohw.

Reviewer

This article was reviewed by peer experts who are not TCP editors.

Author Contributions

Conceptualization: Cho YS, Shin JG; Formal analysis: Cho YS; Investigation: Cho YS, Shin JG; Methodology: Cho YS; Resources: Cho YS; Software: Cho YS; Supervision: Shin JG; Visualization: Cho YS; Writing - original draft: Cho YS; Writing - review & editing: Cho YS, Shin JG.

go.kr/). The disease severity generally appears to be milder and the hospitalization rate is also prone to be lower in pediatric patients in comparison with adults [1]. However, the Center for Disease Control and Prevention (CDC) of the United States reported multisystem inflammation syndrome in children (MIS-C) associated with COVID-19 from a minor group of pediatric patients, which arose from the recent report investigating clusters of children manifesting with multi-organ involved severe inflammation and recent SARS-CoV-2 infection [2-9]. Therefore, a preliminary case definition for MIS-C has been developed by WHO reflecting the clinical and laboratory characteristics and identifying suspected or confirmed cases [10]. Treatment for MIS-C consists of immune modulating drugs such as corticosteroids and immunoglobulin and supportive care for pneumonia, respiratory failure, and sepsis [7,8,9,11].

Medication to treat COVID-19 has not met a demand yet and repurposing drugs with well-established safety are an appealing option. However, several repurposing drugs in particular chloroquine, hydroxychloroquine and lopinavir-ritonavir were investigated for the treatment of COVID-19, and only remdesivir obtained approval from the US Food and Drug Administration for inpatients including children ≥ 12 years old and weighing ≥ 40 kg as well as adults [12-19].

Nafamostat, a potent inhibitor of various serine proteases, was initially authorized as a short-acting anticoagulant and used for the treatment of pancreatitis in Japan and Korea for more than 20 years with a well-established safety profile [20]. Previous studies have established that serine protease inhibitors targeting TMPRSS2, such as nafamostat, can block SARS-CoV-2 entry and has been demonstrated *in vitro* and using animal models [21-23]. It is currently in the clinical trials for the treatment of COVID-19, including a phase 3 clinical trial. In particular, the result of an open-label, randomized phase 2 clinical trial exhibited that in high-risk patients requiring oxygen treatment, nafamostat had a considerably higher recovery and a lower mortality rates in comparison to standard care alone. However, there was no significant discrepancy in time to clinical improvement between nafamostat and standard care [24]. A main route of elimination of nafamostat represents the hydrolytic metabolism to the inactive metabolites such as 6-amino-2-nphthol (AN) and *p*-guanidinobenzoic acid (*p*GBA), mainly through arylesterases and carboxylesterase 2, and thus, the unaltered form of nafamostat is less detectable in urine and feces in *in vitro* or *in vivo* assessment [25-28].

Generally, since pediatric clinical researches are difficult to perform and occur with various ethical issues, pharmacokinetic (PK) modeling and simulation are useful tools to define the risk- benefit ratio of a new drug in pediatric drug development and to allow investigators to determine the personalized precision dosing schemes [29]. Furthermore, the models maximize the utilization of available data and simultaneously minimize the need for unnecessary clinical trials by crossing gaps from adults and supporting efficient clinical trial design [30-33]. Especially as the physiologically-based pharmacokinetic (PBPK) modeling approach in pediatrics takes into account ontogeny of metabolic enzymes and age dependent anatomical and physiological changes, it provides more reliable predictions of plasma drug concentrations for the optimization of the clinical trial design for the recommendation of initial doses in children than traditional allometric scaling [30,34].

This study aims to establish a whole body intravenous PBPK model of nafamostat in adults and to scale down the adult PBPK model to children and provide pediatric exposures of nafamostat for different age groups and suggest an optimal weight-based nafamostat dose in pediatric populations.

Translational and Clinical Pharmacology TCP

METHODS

Software used

PK-Sim software of the Open Systems Pharmacology Suite, version 8.0 was used to develop the PBPK models. Model parameter optimization was achieved using the Monte Carlo algorithm executed in PK-Sim. Clinical data from the publication were extracted and digitized by means of WebPlotDigitizer web-based tool (version 4.5; Ankit Rohatgi, Oakland, CA, USA). Data analysis and graphics were performed with the R programming language version 3.6.2 (R Foundation for Statistical Computing, Seoul, Korea) and R Studio version 1.2.5033 (R Studio, Inc, CA, USA).

Data collection

Owing to the limited availability of relevant clinical data for nafamostat, the PK data was from Chinese healthy volunteers that had been administered three doses (10, 20, and 40 mg) of nafamostat intravenously (i.v.) over 2hr and was only used for model development [35]. There was a specific consideration in the corresponding PBPK model in terms of the PK collection of data, anatomical and physiological features of the subject and the study design as well, i.e., dose and administration intervals. For population simulations, mean patient PBPK models were utilized. By altering anatomical and physiological parameters for 1,000 individuals, a simulated population of a mean PBPK model was generated [36].

PBPK model development in adults

The dose, physicochemical properties, and *in vitro* metabolic elimination that were utilized for the final nafamostat PBPK model in adults are listed in **Table 1**. For the development of adult PBPK model of nafamostat, the information about a) physicochemical properties, b) distribution, metabolism and excretion processes, and c) clinical design for the above mentioned i.v. infusion of nafamostat was obtained and used not only to implement relevant metabolic enzymes but also to inform drug-specific input parameters. Since collected data could not be adequately obtained from the literature, parameter estimation was conducted

Table 1. Nafamostat key parameters for adult PBPK development

Parameters	Initial estimate, unit	Final estimate, unit	Reference/Comment
Basic Physico-chemistry			
Molecular weight	378.38 g/mol	378.38 g/mol	Drug Bank
Lipophilicity (logP)	2.75	2.59	Drug Bank and fitted
Fraction unbound	0.73	0.50	Drug Bank and fitted
pKa	11.32	11.32	Drug Bank
Solubility	0.03 mg/mL	0.03 mg/mL	Drug Bank and fitted
Distribution			
Specific organ permeability	0.004 cm/min	0.004 cm/min	PK-Sim standard
Partition coefficient (blood cells/plasma)	3.85	4.45	Calculated and fitted by PK-Sim
Permeability from blood cell to plasma	0.0047 cm/min	0.0068 cm/min	Calculated and fitted by PK-Sim
Partition coefficient (interstitial/plasma) in muscle	9.03	110.94	Calculated and fitted by PK-Sim
Permeability between plasma and interstitial in muscle	0.02 cm/min	9.97 cm/min	Calculated and fitted by PK-Sim
Metabolism			
Carboxylesterase 2, Km	1,790 μM	1,790 μM	[28]
Carboxylesterase 2, Vmax	26.9 nmol/min/mg protein	26.9 nmol/min/mg protein	[28]
Arylesterase, Km	628 μM	628 μM	[28]
Arylesterase, Vmax	140 nmol/ml/min specific enzyme	140 nmol/ml/min specific enzyme	[28]
Excretion			
Renal clearance: GFR fraction	0.01	0.01	Arbitrary low value
Biliary clearance	0.01 1/min	0.01 1/min	Arbitrary low value

GFR, glomerular filtration.

https://doi.org/10.12793/tcp.2022.30.e4

by fitting the model to observed PK data to acquire valuable input parameters for model. Observed, computed, or assumed parameters were integrated as follows. 1) physicochemical properties of nafamostat such as molecular weight, cLogP, fraction unbound, and blood/plasma ratio values were calculated based on chemical structure (DrugBank, https://go.drugbank.com/). 2) distribution estimation of tissue partition ratio was needed for accurate reproduction of disposition PK profile. Nafamostat typically exhibits two compartment distribution profile. However, The PK profile implemented by the initial estimated parameter showed one compartment distribution. To fit to the observed PK profile, we modified and optimized the partition coefficient and permeability of the muscle, one of the major large organs which can affect distribution of PK but is not the infection site to influence to efficacy of the drug. In addition, the parameters for distribution between blood cell and plasma, i.e., partition coefficient (blood cells/plasma) and permeability from blood cell to plasma, were also modulated to finetune to the PK profile, which the final estimates of them were not considerably deviated. 3) *in vitro* kinetic data for metabolism of nafamostat via carboxylesterase2 and arylesterase was inputed to recover observed nafamostat area under the concentration-time curve (AUC). The PK Sim expression data was used to inform tissue expression distribution of the implemented metabolic enzymes [37]. Since PK-Sim does not provide information about tissue specific expression for subtype of carboxylesterase, we incorporate the kinetic parameters into the integrated carboxylesterase process. The literature did not report the subtype of arylesterase, i.e., paraoxonase 1 and 2 (PON1 and 2), involved in metabolism of nafamostat. With this limitation, the kinetic parameters were evenly incorporated into two subtypes of arylesterase. 4) nafamostat is transported by organic cation transporters (OCTs) in the basolateral membrane of proximal tube. However, it harbors a short plasma half-life owing to high hydrolytic metabolism and activities of OCTs for nafamostat in kidney are not expected to result in significant changes in nafamostat plasma exposure. Because of this, OCTs transport for nafamostat was not incorporated into the model and the exclusion of this disposition mechanism are not anticipated to considerably affect predicted pediatric nafamostat exposure. 5) As only negligible levels of the parent nafamostat can be detected in urine and feces, arbitrary low values of renal or biliary excretion parameters were incorporated into the model.

Pediatric scaling and model application

The model was scaled to adolescent, child, young child, infant, and neonate for prediction of PK in the respective populations after the establishment of the adult PBPK model. Each age group was defined as follows: Neonate (–4 weeks postnatal age), Infant (4 weeks–2 years postnatal age), Young child (2–6 years), Child (6–12 years), Adolescent (12–18 years), Adult (18–45 years). To build the pediatric PBPK model, both anthropometric and physiologic parameters, as well as tissue concentration of metabolic enzymes, were scaled to values of the corresponding key population explaining age-dependent changes. In particular, the composition and size of tissue compartments, maturation and protein binding of elimination process are all factors to consider. Since there is no ontogeny function currently presenting for arylesterases and carboxylesterase 2 in PK-Sim, the ontogeny patterns for activities of the enzymes was found in published literature and applied to the PK-Sim platform [38,39]. Plasma concentration-time profiles in pediatric populations was simulated subsequently by using the extrapolated PBPK model. To compare the effect of the PK prediction using the pediatric PBPK models, a typical allometric scaling approach was used. Here, the clearance was scaled by allometry from adults to the pediatric populations with exponent of 0.75 and normalized to the body weight of 56.4 kg, the mean body weight in simulation data used for the adult PBPK model development, as follows.

https://doi.org/10.12793/tcp.2022.30.e4

PBPK model evaluation

Due to the scarcity of PK data from pediatric population, only adult PBPK models were evaluated using the following approaches. In goodness-of-fit plots, the predicted plasma concentrations and their corresponding observed values were compared. Furthermore, the observed plasma concentration-time profiles from adult were visually compared to the predicted plasma PK profile from PBPK models. To predict the variability of plasma PK profile, virtual populations of 100 individuals representing the respective clinical trial population were created. The predictions of population were plotted as median with 95% prediction interval. The geometric mean fold errors (GMFE) of AUC and maximum plasma concentration (C_{max}) ratios were calculated. As a reference, a two-fold error range from the observed values for model predictions was taken. Such a range is considered appropriate for a predicted model and also commonly reported by other investigators [40-42].

RESULTS

Adult PBPK model development and evaluation

Following a thorough review of the literature, two PK studies in healthy adults with i.v. administration of the same dosages were identified [43,44]. However, their exposures were different, up to around two-fold, due to a different quantitative method. We selected the more recently published PK study, which was performed in 30 Chinese healthy subjects and quantified by liquid chromatography-mass spectrometry (LCMS). A Japanese population model of PK-Sim was used for simulating adult PK profiles and exposure as the Japanese were considered a more closely related ethnic group for the respective real population, i.e., Chinese, in the population model provided by PK-Sim. To match the observed clinical study, 100 virtual subjects with ages ranging from 20 to 26 years and an equal portion of males and females were simulated. The whole-body adult PBPK model adequately predicted plasma concentration-time profiles of nafamostat following i.v. administration. Visual comparisons of the predicted to observed plasma PK profiles are depicted in **Fig. 1**. The goodness-of-fit of predicted versus observed plasma concentrations is illustrated in **Fig. 2**. The GMFE values for the adult PBPK model were 1.65 and 1.21 for AUC and C_{max}, respectively. Furthermore, 100% of all predicted plasma concentrations fall within two-fold of the respective observed concentrations. The PBPK model predictions for the fraction of nafamostat metabolism was ~99% and the unchanged fraction excreted in urine or feces was negligible, which is in concordance with the literature [25-28]. Two factors for tissue distribution of nafamostat were estimated in order to more accurately describe observed disposition profile of it.

Pediatric PBPK model development by scaling the adult model

The adult PBPK model was scaled to predict pediatric exposure of nafamostat after i.v. administration of the highest weight-based dosing regimen being used in an adult phase II and III study, 0.2 mg/kg/h during 14 days. This is because 0.2 mg/kg/h is the approved dose of nafamostat for disseminated intravascular coagulation (DIC) and acute pancreatitis and has been broadly well tolerated in clinical trials [20,24]. The model predicted the exposure of nafamostat according to six different age groups as depicted in **Fig. 3**. As age advances from neonate to adult, AUC and C_{max} of nafamostat slightly increased from neonate to infant, continuously decreased to child with nadir, and then increased from child to adult. The fold change of predicted AUC for the respective pediatric groups over those of adults after the administration of the same weight based dosing regimen were 0.88, 0.92, 0.85, 0.78, and 0.92 for neonate, infant, young child, child, and adolescent subjects, respectively. The

https://doi.org/10.12793/tcp.2022.30.e4

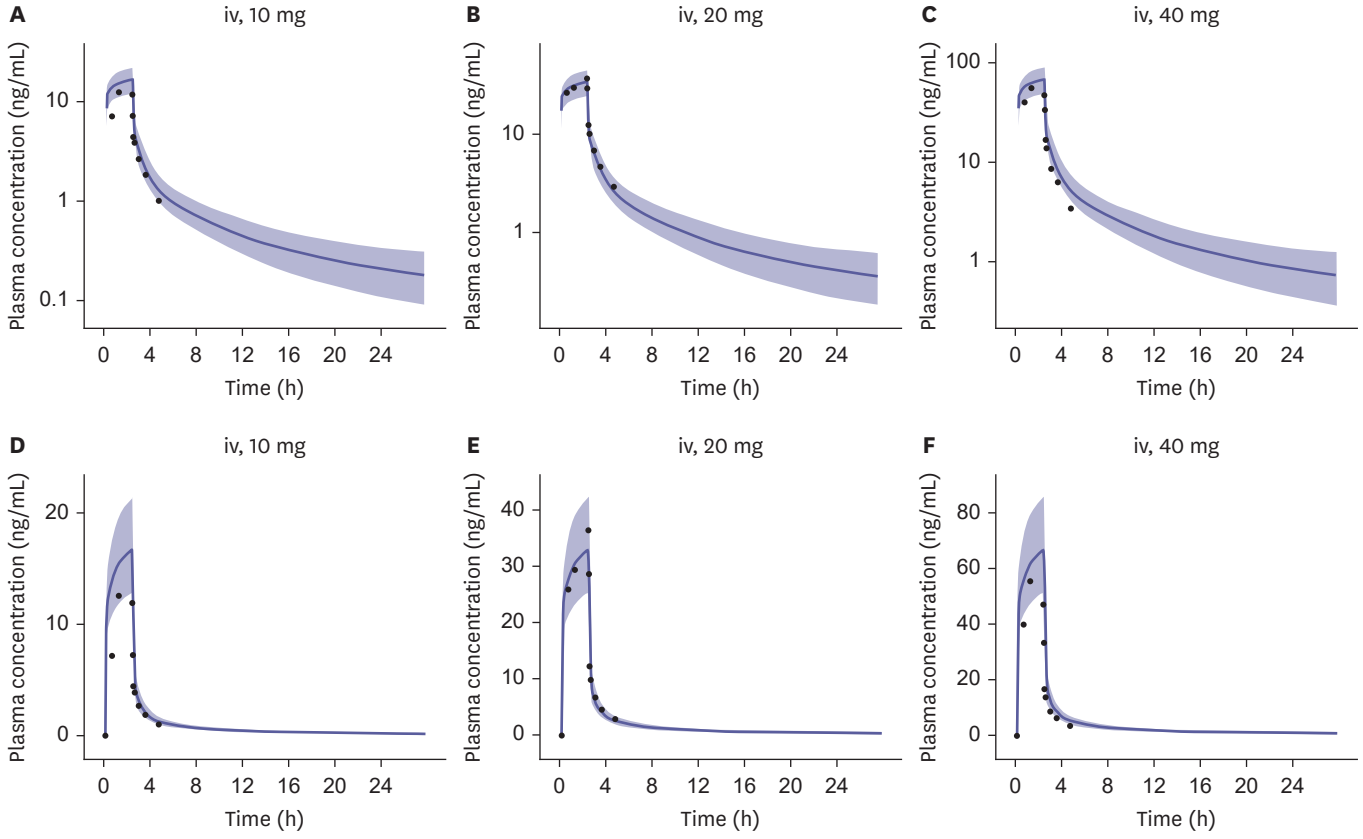

Figure 1. The predicted and observed plasma concentration-time profile after intravenous nafamostat administration in adults with semi-log scale (A-C) and linear scale (D-F): a single dose of intravenous administration of 10, 20, and 40 mg, respectively. Population simulations (n = 100) are shown as line with shaded areas, which represents median and 95% prediction interval, respectively. Observed data are shown as points.
iv, intravenous.

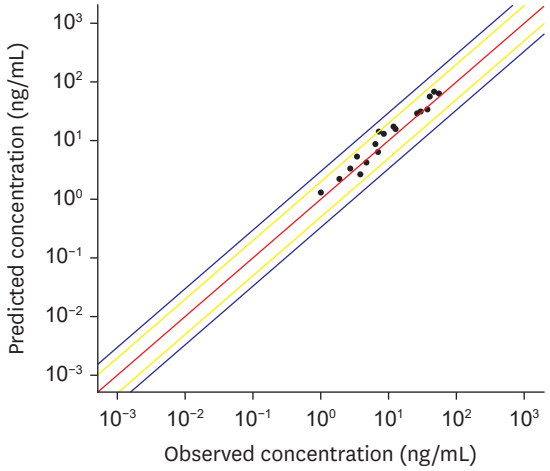

Figure 2. The goodness-of-fit plot after intravenous nafamostat administration in adults. Predicted versus observed plasma concentrations are displayed. Each point represents a single plasma concentration. Red line indicates the line of identity. Yellow and blue line mark 2-fold and 3-fold deviation, respectively.

fold change of predicted C_{max} for the respective pediatric group over those of adults after the administration of the same weight-based dosing regimen were 0.87, 0.92, 0.84, 0.78, and 0.92 for neonate, infant, young child, child, and adolescent subjects, respectively

https://doi.org/10.12793/tcp.2022.30.e4

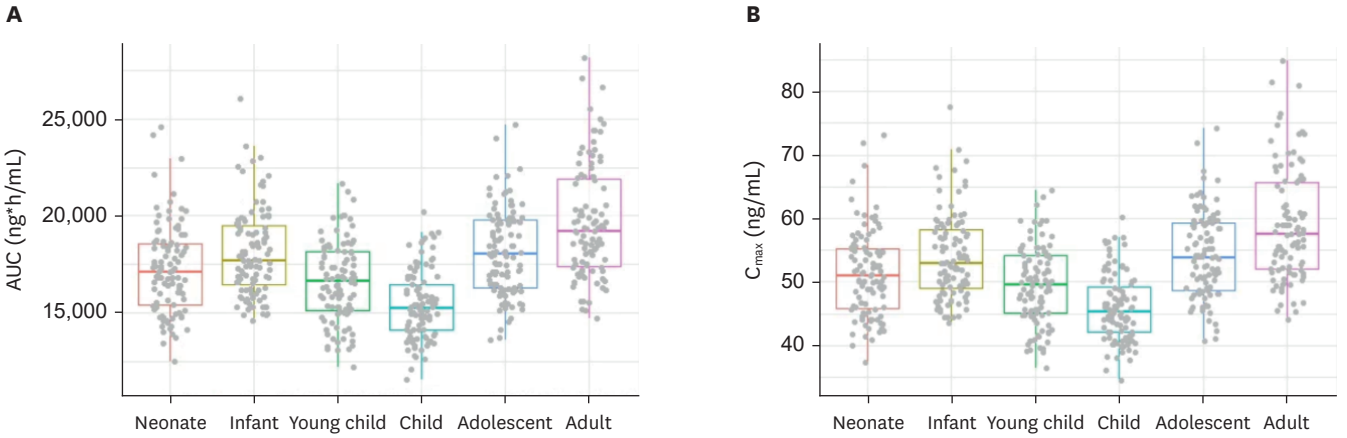

Figure 3. The predicted exposure after intravenous nafamostat administration of 0.2 mg/kg/h during 14 days in six different age groups. AUC (A) and C_{max} (B) predicted by the physiologically-based pharmacokinetic model scaled from the adult population. Gray closed circles are predicted exposure values of simulated individual virtual subjects. Horizontal lines represent the median, with the top and the bottom of the boxes representing the first and third quantiles (IQR), whiskers indicate the extreme data within 1.5 × IQR.
AUC, area under the curve; C_{max}, maximum plasma concentration; IQR, interquartile range.

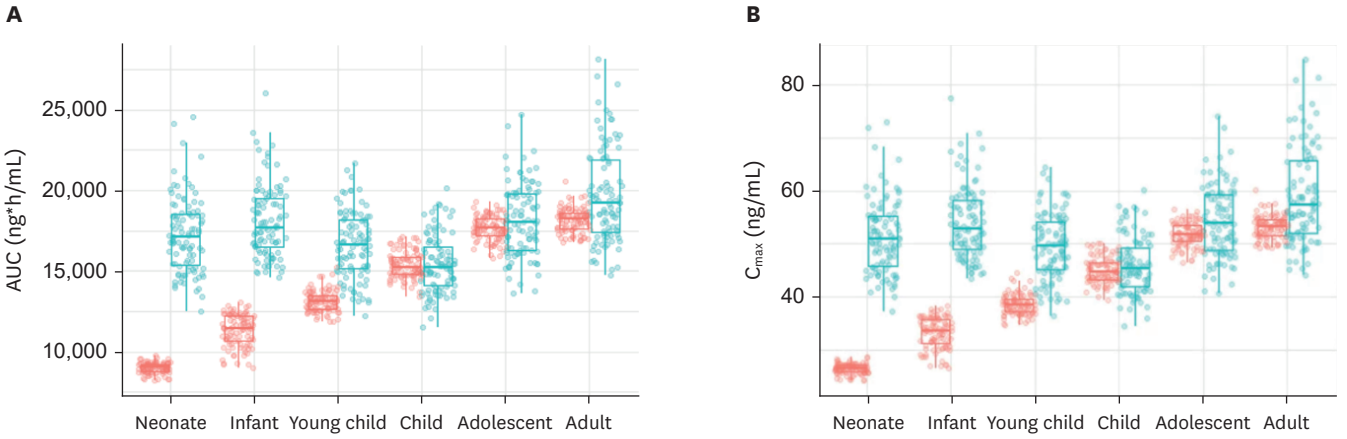

Figure 4. The comparison between AUC (A) and C_{max} (B) predicted by allometry and the PBPK model after intravenous nafamostat administration of 0.2 mg/kg/h during 14 days in six different age groups. Red boxes and points indicate AUC (A) and C_{max} (B) predicted by allometry, blue boxes and points indicate AUC (A) and C_{max} (B) predicted by the PBPK model. Open circles are predicted AUC (A) and C_{max} (B) values of individual simulated virtual subjects. Horizontal lines represent the median, with the top and the bottom of the boxes representing the first and third quantiles (IQR), whiskers indicate the extreme data within 1.5 × IQR.
AUC, area under the curve; C_{max}, maximum plasma concentration; IQR, interquartile range.

Comparison of pediatric exposures predicted by PBPK and allometry

A classical allometric scaling approach was used (body weight exponent = 0.75) to predict pediatric AUC and C_{max} of nafamostat and directly compare with those predicted by the PBPK model. As shown in **Fig. 4**, we found that both methodologies predicted similarly for adult, adolescent, and child subjects, whereas there is a remarkable deviation between PBPK and allometry prediction in neonate, infant, and young child subjects.

DISCUSSION

As the COVID-19 pandemic is rapidly outspreading and the number of pediatric patients is gradually growing, severe cases for children such as MIS-C are being reported [2-9,45]. However, studies that have investigated pharmacotherapy for the COVID-19 treatment

https://doi.org/10.12793/tcp.2022.30.e4

have been performed mostly in adults [46]. Nafamostat is currently being explored for the treatment of COVID-19 in adults and the data that support its exposure in children remain limited. The unmet medical need for providing nafamostat as a therapeutic option in pediatrics demand the use of PBPK modeling and simulation to optimize pharmacotherapies.

In this study, PBPK models of nafamostat for an adult population have been successfully developed. The model provides a consistent representation of dose-exposure relationship following i.v. administration of a dose range and adequately describes plasma concentration-time profiles of nafamostat. More importantly, by scaling the adult PBPK model to pediatrics, we delineate the potential of PBPK modeling approach to more reasonably predict PK in children.

Nafamostat is unstable in plasma and a highly polar drug with few practical methods for its *in vivo* quantification and only an insufficient number of PK studies with valid nafamostat concentration measurements available [43,44,47]. In the same context, the recent randomized controlled study exploring safety and PK/pharmacodynamics reported that the majority of patients exhibited undetectable levels of nafamostat [unpublished data]. We selected a PK study quantified using LCMS rather than a radioisotope-labeling method which often overestimates the parent drug because the metabolites also consist of radioisotope, particularly for unstable compounds. The adult PBPK model was first established using a PK study of i.v. administration of three doses (10, 20, and 40 mg). The kinetic parameters for nafamostat metabolism were input using *in vitro* experimental data from the literature and several parameters were fitted utilizing population means of the PK study. The resulting adult PBPK model was able to predict nafamostat exposure reliably over a dose range, indicating that the crucial processes driving nafamostat PK were adequately captured. The initial establishment of the model in adults offered a modeling strategy that served as a solid foundation for age extrapolation to improve accuracy of the pediatric model predictions.

Based on the concept of defining absorption, distribution, metabolism and excretion as a function of anatomy, physiology, and biochemical reaction, PBPK modeling and simulation provides the chance of reasonable scaling between adults and pediatrics. Such a strategy is prevalent in the establishment of models in children and is already utilized by other investigators [41-42, 48]. This study defined six different age groups for predictions of pediatric clearance. Based on the information, including size change and ontogeny of metabolic enzyme of nafamostat, i.e., arylesterases and carboxylesterase 2, the exposures foreach pediatric group was predicted using a virtual population of 100 individuals from that age category. As PK-Sim does not currently equip an ontogeny function for arylesterases and carboxylesterase 2, it was user-provided from the literature and integrated into PK-Sim [38,39]. In the case of microsomal carboxylesterase 2, its expression increases across the three consecutive age groups, which are children from birth to 3 weeks, between 3 weeks and 6 years, and over 6 years [38]. In the case of arylesterases, its activity continuously increases from birth to 7 years [39]. As age increases, the predicted nafamostat exposures are slightly raised from neonate to infant followed by a steady decrease from infant to child, and then increased from child to adult, as shown in **Fig. 3**. Whereas the predicted exposures of child subjects were 0.78 fold lower than those of adults, the predicted exposures of all other pediatric groups fell within 0.85 fold when compared to those of adults, indicating the pediatric exposures predicted by PBPK model are not substantially different from those of adults. Based on these finding, we cautiously may recommend a weight based initial dosing regimen for each age group. Assuming 0.2 mg/kg/h currently approved for DIC and acute pancreatitis and being conducted in a clinical trial for COVID-19 is suitable for adults,

for neonate, infant, young child, child, and adolescent subjects, the adult dosage regimen is likely to be increased with 0.23 mg/kg/h, 0.22 mg/kg/h, 0.24 mg/kg/h, 0.25 mg/kg/h, and 0.22 mg/kg/h, respectively. For child subjects, the largest dose changes relative to the adult dosage regimen may be considered. Considering nafamostat is primarily eliminated by metabolism, pediatric clearance can be determined by size as well as maturation of the metabolic enzyme, i.e., arylesterases and carboxylesterase 2. In pediatric PBPK models, most efforts have been contributed to the incorporation of age-dependent changes in metabolic clearance. Especially for the enzyme cytochrome P450s (CYP) developmental patterns and clearance of drugs mainly metabolized by these enzymes are relatively well documented [49]. Generally, because of differences in enzyme levels, drugs highly metabolized are administered at a higher mg/kg dose in young child compared with newborns, which was consistent in the case of nafamostat [50]. The hepatic clearance of the drugs can be higher in infants and child as liver blood flow is increased in comparison with adults due to the increased ratio of liver to total body mass in the preceding group [51]. Thus, drugs primarily metabolized in the liver are likely to exhibit a lower exposure rate compared to adults. Similarly, in nafamostat, the predicted exposure of infants, young child, and child were lower than that of adults.

The selection of dose in pediatric populations is generally obtained from adult PK data through two common approaches, PBPK and allometric scaling [52-54]. In this study, we delineated nafamostat AUC in pediatric patients based on a PBPK model and compared the results from allometric scaling. The comparison analysis indicated that there was a notable separation in predicted pediatric exposure between the methods in neonate, infant, and young child populations, while those of adult, adolescent, and child subjects coincided between them. Generally, PBPK models explain enzyme ontogeny and age dependent alteration in organ development and function. Therefore, they can provide more reliable prediction of plasma drug concentrations [30,52]. Allometric scaling does not account for drug specific disposition mechanisms, instead extrapolating exposure based on body size and fixed exponent (usually 0.75), which can result in large overestimations of metabolic clearance in very young children due to their immature enzymes, which is in line with our finding [30,34]. When compared to simple allometry, PBPK models tend to predict higher exposures in younger children. Therefore, PBPK models present more conventional predictions with respect to safety.

This study had several limitations. First, since available PK studies with valid nafamostat concentrations were limited, we utilized only one study using three dosages for establishing the PBPK model and did not validate the model. Second, our recommended pediatric dosing regimen assumes that the exposure-response relationship in pediatric populations will be similar to that of adults and can be rationally extrapolated from adults. Third, owing to the scarcity of available observed pediatric PK data of nafamostat, the predictive performance of the PBPK model could not be verified.

Our study provides reasonable evidence to recommend a nafamostat weight-based dosing regimen with efficacious exposure in pediatric COVID-19 patients. A PBPK model has been established that adequately captures the observed PK profile of nafamostat in adult healthy volunteers. By scaling this model to pediatric populations, the pediatric exposures of nafamostat were predicted and reasonable pediatric doses were cautiously recommended, aiding future investigations of nafamostat PKs in pediatric populations, including the design of clinical trials and precision dosing.

https://doi.org/10.12793/tcp.2022.30.e4

ACKNOWLEDGMENTS

We appreciate Nguyen Thi Van Anh who is a graduate student in Inje University College of Medicine for her English editing.

REFERENCES

1. Wang E, Brar K. COVID-19 in children: an epidemiology study from China. J Allergy Clin Immunol Pract 2020;8:2118-2120.
PUBMED | CROSSREF
2. Centers for Disease Control and Prevention. Multisystem Inflammatory Syndrome in Children (MIS-C) Associated with Coronavirus Disease 2019 (COVID-19) [Internet]. https://emergency.cdc.gov/han/2020/han00432.asp. Accessed February 5, 2022.
3. Riphagen S, Gomez X, Gonzalez-Martinez C, Wilkinson N, Theocharis P. Hyperinflammatory shock in children during COVID-19 pandemic. Lancet 2020;395:1607-1608.
PUBMED | CROSSREF
4. Verdoni L, Mazza A, Gervasoni A, Martelli L, Ruggeri M, Ciuffreda M, et al. An outbreak of severe Kawasaki-like disease at the Italian epicentre of the SARS-CoV-2 epidemic: an observational cohort study. Lancet 2020;395:1771-1778.
PUBMED | CROSSREF
5. Toubiana J, Poirault C, Corsia A, Bajolle F, Fourgeaud J, Angoulvant F, et al. Kawasaki-like multisystem inflammatory syndrome in children during the covid-19 pandemic in Paris, France: prospective observational study. BMJ 2020;369:m2094.
PUBMED | CROSSREF
6. Pouletty M, Borocco C, Ouldali N, Caseris M, Basmaci R, Lachaume N, et al. Paediatric multisystem inflammatory syndrome temporally associated with SARS-CoV-2 mimicking Kawasaki disease (Kawa-COVID-19): a multicentre cohort. Ann Rheum Dis 2020;79:999-1006.
PUBMED | CROSSREF
7. Feldstein LR, Rose EB, Horwitz SM, Collins JP, Newhams MM, Son MB, et al. Multisystem inflammatory syndrome in U.S. children and adolescents. N Engl J Med 2020;383:334-346.
PUBMED | CROSSREF
8. Chao JY, Derespina KR, Herold BC, Goldman DL, Aldrich M, Weingarten J, et al. Clinical characteristics and outcomes of hospitalized and critically ill children and adolescents with coronavirus disease 2019 at a tertiary care medical center in New York City. J Pediatr 2020;223:14-19.e2.
PUBMED | CROSSREF
9. Chiotos K, Bassiri H, Behrens EM, Blatz AM, Chang J, Diorio C, et al. Multisystem inflammatory syndrome in children during the coronavirus 2019 pandemic: a case series. J Pediatric Infect Dis Soc 2020;9:393-398.
PUBMED | CROSSREF
10. World Health Organization. Multisystem inflammatory syndrome in children and adolescents temporally related to COVID-19 [Internet]. https://www.who.int/news-room/commentaries/detail/multisystem-inflammatory-syndrome-in-children-and-adolescents-with-covid-19. Accessed July 17, 2020.
11. Centers for Disease Control and Prevention. Information for clinicians on investigational therapeutics for patients with COVID-19 [Internet]. https://www.cdc.gov/coronavirus/2019-ncov/hcp/therapeutic-options.html. Accessed July 17, 2020.
12. Self WH, Semler MW, Leither LM, Casey JD, Angus DC, Brower RG, et al. Effect of Hydroxychloroquine on clinical status at 14 days in hospitalized patients with Covid-19: a randomized clinical trial. JAMA 2020;324:2165-2176.
PUBMED | CROSSREF
13. Cavalcanti AB, Zampieri FG, Rosa RG, Azevedo LC, Veiga VC, Avezum A, et al. Hydroxychloroquine with or without azithromycin in mild-to-moderate Covid-19. N Engl J Med 2020;383:2041-2052.
PUBMED | CROSSREF
14. Cao B, Wang Y, Wen D, Liu W, Wang J, Fan G, et al. A trial of lopinavir-ritonavir in adults hospitalized with severe Covid-19. N Engl J Med 2020;382:1787-1799.
PUBMED | CROSSREF
15. Beigel JH, Tomashek KM, Dodd LE, Mehta AK, Zingman BS, Kalil AC, et al. Remdesivir for the treatment of Covid-19 - final report. N Engl J Med 2020;383:1813-1826.
PUBMED | CROSSREF

16. Horby P, Lim WS, Emberson JR, Mafham M, Bell JL, Linsell L, et al. Dexamethasone in hospitalized patients with Covid-19. N Engl J Med 2021;384:693-704.
PUBMED | CROSSREF

17. U.S. Food & Drug Administration. FDA Approves First Treatment for COVID-19 [Internet]. https://www.fda.gov/news-events/press-announcements/fda-approves-first-treatment-covid-19. Accessed December 8, 2020.

18. Gilead. Gilead announces approval of Veklury (remdesivir) in Japan for patients with severe COVID-19 [Internet]. https://www.gilead.com/news-and-press/press-room/press-releases/2020/5/gilead-announces-approval-of-veklury-remdesivir-in-japan-for-patients-with-severe-covid19. Accessed July 17, 2020.

19. Gilead. European commission grants conditional marketing authorization for Gilead's Veklury (remdesivir) for the treatment of COVID-19 [Internet]. https://www.gilead.com/news-and-press/press-room/press-releases/2020/7/european-commission-grants-conditional-marketing-authorization-for-gileads-veklury-remdesivir-for-the-treatment-of-covid19. Accessed July 17, 2020.

20. Sundaram S, Gikakis N, Hack CE, Niewiarowski S, Edmunds LH Jr, Koneti Rao A, et al. Nafamostat mesilate, a broad spectrum protease inhibitor, modulates platelet, neutrophil and contact activation in simulated extracorporeal circulation. Thromb Haemost 1996;75:76-82.
PUBMED | CROSSREF

21. Yamaya M, Shimotai Y, Hatachi Y, Lusamba Kalonji N, Tando Y, Kitajima Y, et al. The serine protease inhibitor camostat inhibits influenza virus replication and cytokine production in primary cultures of human tracheal epithelial cells. Pulm Pharmacol Ther 2015;33:66-74.
PUBMED | CROSSREF

22. Hoffmann M, Schroeder S, Kleine-Weber H, Müller MA, Drosten C, Pöhlmann S. Nafamostat mesylate blocks activation of SARS-CoV-2: new treatment option for COVID-19. Antimicrob Agents Chemother 2020;64:e00754-e20.
PUBMED | CROSSREF

23. Li K, Meyerholz DK, Bartlett JA, McCray PB Jr. The TMPRSS2 inhibitor nafamostat reduces SARS-CoV-2 pulmonary infection in mouse models of COVID-19. MBio 2021;12:e0097021.
PUBMED | CROSSREF

24. Zhuravel SV, Khmelnitskiy OK, Burlaka OO, Gritsan AI, Goloshchekin BM, Kim S, et al. Nafamostat in hospitalized patients with moderate to severe COVID-19 pneumonia: a randomised Phase II clinical trial. EClinicalMedicine 2021;41:101169.
PUBMED | CROSSREF

25. Aoyama T, Okutome T, Nakayama T, Yaegashi T, Matsui R, Nunomura S, et al. Synthesis and structure-activity study of protease inhibitors. IV. Amidinonaphthols and related acyl derivatives. Chem Pharm Bull (Tokyo) 1985;33:1458-1471.
PUBMED | CROSSREF

26. Yang H, Henkin J, Kim KH, Greer J. Selective inhibition of urokinase by substituted phenylguanidines: quantitative structure-activity relationship analyses. J Med Chem 1990;33:2956-2961.
PUBMED | CROSSREF

27. Nanpo T, Ohtsuki T, Jin Y, Matsunaga K, Takahashi M, Shibuya M, et al. Pharmacokinetic study of FUT-175 (nafamostat mesylate) (1)-blood level profiles, tissue distribution, metabolism and excretion in rats after intravenous administration. Clin Rep 1984;18:467-488.

28. Yamaori S, Fujiyama N, Kushihara M, Funahashi T, Kimura T, Yamamoto I, et al. Involvement of human blood arylesterases and liver microsomal carboxylesterases in nafamostat hydrolysis. Drug Metab Pharmacokinet 2006;21:147-155.
PUBMED | CROSSREF

29. Ward RM, Sherwin CM. Ethics of drug studies in the newborn. Paediatr Drugs 2015;17:37-42.
PUBMED | CROSSREF

30. Lin W, Heimbach T, Jain JP, Awasthi R, Hamed K, Sunkara G, et al. A physiologically based pharmacokinetic model to describe artemether pharmacokinetics in adult and pediatric patients. J Pharm Sci 2016;105:3205-3213.
PUBMED | CROSSREF

31. Germovsek E, Barker CI, Sharland M, Standing JF. Pharmacokinetic-Pharmacodynamic modeling in pediatric drug development, and the importance of standardized scaling of clearance. Clin Pharmacokinet 2019;58:39-52.
PUBMED | CROSSREF

32. Conklin LS, Hoffman EP, van den Anker J. Developmental pharmacodynamics and modeling in pediatric drug development. J Clin Pharmacol 2019;59 Suppl 1:S87-S94.
PUBMED | CROSSREF

33. Mulugeta YL, Zajicek A, Barrett J, Sachs HC, McCune S, Sinha V, et al. Development of drug therapies for newborns and children: the scientific and regulatory imperatives. Pediatr Clin North Am 2017;64:1185-1196.
PUBMED | CROSSREF

34. Calvier EA, Krekels EH, Johnson TN, Rostami-Hodjegan A, Tibboel D, Knibbe CA. Scaling drug clearance from adults to the young children for drugs undergoing hepatic metabolism: a simulation study to search for the simplest scaling method. AAPS J 2019;21:38.
PUBMED | CROSSREF

35. Cao YG, Zhang M, Yu D, Shao JP, Chen YC, Liu XQ. A method for quantifying the unstable and highly polar drug nafamostat mesilate in human plasma with optimized solid-phase extraction and ESI-MS detection: more accurate evaluation for pharmacokinetic study. Anal Bioanal Chem 2008;391:1063-1071.
PUBMED | CROSSREF

36. Willmann S, Höhn K, Edginton A, Sevestre M, Solodenko J, Weiss W, et al. Development of a physiology-based whole-body population model for assessing the influence of individual variability on the pharmacokinetics of drugs. J Pharmacokinet Pharmacodyn 2007;34:401-431.
PUBMED | CROSSREF

37. Open Systems Pharmacology Suite Community Open Systems Pharmacology Suite Manual. Version 7.4. [Internet] https://github.com/Open-Systems-Pharmacology/OSPSuite.Documentation/blob/master/Open%20Systems%20Pharmacology%20Suite.pdf. Accessed March 25, 2020.

38. Hines RN, Simpson PM, McCarver DG. Age-dependent human hepatic carboxylesterase 1 (CES1) and carboxylesterase 2 (CES2) postnatal ontogeny. Drug Metab Dispos 2016;44:959-966.
PUBMED | CROSSREF

39. Huen K, Harley K, Brooks J, Hubbard A, Bradman A, Eskenazi B, et al. Developmental changes in PON1 enzyme activity in young children and effects of PON1 polymorphisms. Environ Health Perspect 2009;117:1632-1638.
PUBMED | CROSSREF

40. Ginsberg G, Hattis D, Russ A, Sonawane B. Physiologically based pharmacokinetic (PBPK) modeling of caffeine and theophylline in neonates and adults: implications for assessing children's risks from environmental agents. J Toxicol Environ Health A 2004;67:297-329.
PUBMED | CROSSREF

41. Edginton AN, Schmitt W, Willmann S. Development and evaluation of a generic physiologically based pharmacokinetic model for children. Clin Pharmacokinet 2006;45:1013-1034.
PUBMED | CROSSREF

42. Parrott N, Davies B, Hoffmann G, Koerner A, Lave T, Prinssen E, et al. Development of a physiologically based model for oseltamivir and simulation of pharmacokinetics in neonates and infants. Clin Pharmacokinet 2011;50:613-623.
PUBMED | CROSSREF

43. Cao YG, Chen YC, Hao K, Zhang M, Liu XQ. An *in vivo* approach for globally estimating the drug flow between blood and tissue for nafamostat mesilate: the main hydrolysis site determination in human. Biol Pharm Bull 2008;31:1985-1989.
PUBMED | CROSSREF

44. Abe T, Kinoshita T, Matsuda J, Ogushi T, Kawasugi K, Yoshimura Y, et al. Phase one study of FUT-175, single and multiple dose study. Jpn Pharmacol Ther 1984;12:4941-4964.

45. Zachariah P, Johnson CL, Halabi KC, Ahn D, Sen AI, Fischer A, et al. Epidemiology, clinical features, and disease severity in patients with coronavirus disease 2019 (COVID-19) in a children's hospital in New York City, New York. JAMA Pediatr 2020;174:e202430.
PUBMED | CROSSREF

46. Watt KM. How to rapidly determine first-in-children dosing for COVID-19 therapeutics. JAMA Pediatr 2020;174:e202435.
PUBMED | CROSSREF

47. Aoyama T, Sasaki H, Shibuya M, Suzuki Y. Spectrofluorometric determination of FUT-175 (nafamstat mesilate) in blood based on trypsin-inhibitory activity. Chem Pharm Bull (Tokyo) 1985;33:2142-2144.
PUBMED | CROSSREF

48. Kersting G, Willmann S, Würthwein G, Lippert J, Boos J, Hempel G. Physiologically based pharmacokinetic modelling of high- and low-dose etoposide: from adults to children. Cancer Chemother Pharmacol 2012;69:397-405.
PUBMED | CROSSREF

49. Verscheijden LF, Koenderink JB, Johnson TN, de Wildt SN, Russel FG. Physiologically-based pharmacokinetic models for children: starting to reach maturation? Pharmacol Ther 2020;211:107541.
PUBMED | CROSSREF

50. Batchelor HK, Marriott JF. Paediatric pharmacokinetics: key considerations. Br J Clin Pharmacol 2015;79:395-404.
PUBMED | CROSSREF

51. Gibbs JP, Murray G, Risler L, Chien JY, Dev R, Slattery JT. Age-dependent tetrahydrothiophenium ion formation in young children and adults receiving high-dose busulfan. Cancer Res 1997;57:5509-5516.
PUBMED

52. Strougo A, Eissing T, Yassen A, Willmann S, Danhof M, Freijer J. First dose in children: physiological insights into pharmacokinetic scaling approaches and their implications in paediatric drug development. J Pharmacokinet Pharmacodyn 2012;39:195-203.
PUBMED | CROSSREF

53. Malik PR, Edginton AN. Physiologically-based pharmacokinetic modeling vs. allometric scaling for the prediction of infliximab pharmacokinetics in pediatric patients. CPT Pharmacometrics Syst Pharmacol 2019;8:835-844.
PUBMED | CROSSREF

54. Edginton AN. Knowledge-driven approaches for the guidance of first-in-children dosing. Paediatr Anaesth 2011;21:206-213.
PUBMED | CROSSREF